OPTIMAL CONTROL OF 6-DOF ELECTROMAGNETIC FORMATION USING THE LEGENDRE PSEUDOSPECTRAL METHOD

Jing CHEN[(1)], Xiaokui YUE[(2)], Peng LI[(3)]
[(1)(2)(3)]*National Key Laboratory of Aerospace Flight Dynamics, Northwestern Polytechnical University, Xi'an 710072, China,*

(1)+86 159 3488 5855,mirandachanj@gmail.com
(2)+86 13571818923, xkyue@nwpu.edu.cn
(3)+86 13991205708, SatLi@mail.nwpu.edu.cn

Abstract: *Interest in the electromagnetic formation flying has prompt studies of highly coupled, nonlinear and constrained dynamics of relative translational and rotational motion. Due to the fact that both electromagnetic forces and torques are determined by relative position and attitude of the array, a 6-DOF model is established to fully utilize the coupling effects. Reconfiguration of EMFF is an optimal control problem and can be transformed into constrained non-linear program through the Legendre pseudospectral method. A high-precision numerical computation method is used to generate optimal trajectories. The simulation results verify the validity of the optimization method and its algorithm.*

Keywords: *Electromagnetic Formation Flying, 6-DOF Relative Motion Model, the Legendre Pseudospectral Method.*

1. Introduction

Satellite formation flying is an enabling technology distinguished for its high performance. Electromagnetic Formation Flying (EMFF) [1]-[4] is a novel concept which uses High Temperature Superconducting (HTS) coils to provide forces and torques, in order to enable 6 Degree-of-Freedom (DOF) control while avoiding problems posed by the expenditure of propellant. With EMFF powered by solar energy, the life-span is independent of consumables, in exchange of a highly coupled and nonlinear dynamics model.

The system of electromagnets, viz. orthogonal coils, in concert with Reaction Wheels (RWs), can act as simultaneous 6-DOF actuators. The feature that both magnitude and orientation of the Electromagnetic (EM) force is determined by magnetic dipole strength and relative DOF of the array is unique. Another aspect of EMFF is that whenever a shear EM force acts, a shear torque is introduced. The reconfiguration of EMFF is a nonlinear and constrained optimal control problem [9] with regard to both maneuver time and Angular Momentum Management (AMM). Here the Legendre Pseudospectral Method (LPM), as well as its high-precision numerical computation method, is used to generate optimal trajectories for formation reconfiguration.

2. Electromagnetic Dynamics

2.1 Far-Field Model

Assuming that both the chief and the deputy satellites orbiting in space where the effects of geomagnetic field can be ignored. The magnetic moment of the i^{th} satellite $\boldsymbol{\mu}_i = [\mu_{i1}, \mu_{i2}, \mu_{i3}]^{\mathrm{T}}$ is expressed in the LVLH frame. The mounting coordinate is fixed to the satellite's body coordinate; hence the dependence of magnetic force on relative attitude is implicitly embedded in the dipole strength. The far-field model is an approximation of the magnetic field and gives accurate result only when the relative distance is greatly beyond the radius of coils. The magnetic force acted on the i^{th} satellite due to the j^{th} satellite is written as:

$$\mathbf{F}_{ij} = \frac{3\mu_0}{4\pi}[-\frac{5(\boldsymbol{\mu}_i \cdot \mathbf{r}_{ij})(\boldsymbol{\mu}_j \cdot \mathbf{r}_{ij})}{r_{ij}^7}\mathbf{r}_{ij} + \frac{(\boldsymbol{\mu}_i \cdot \mathbf{r}_{ij})}{r_{ij}^5}\boldsymbol{\mu}_j + \frac{(\boldsymbol{\mu}_j \cdot \mathbf{r}_{ij})}{r_{ij}^5}\boldsymbol{\mu}_i + \frac{(\boldsymbol{\mu}_i \cdot \boldsymbol{\mu}_j)}{r_{ij}^5}\mathbf{r}_{ij}] \tag{1}$$

where $\mu_0 = 4\pi \times 10^{-7} H/m$ is the vacuum magnetic permeability. The reaction force is:

$$\mathbf{F}_{ji} = -\mathbf{F}_{ij} \tag{2}$$

Satellites in EMFF can be regarded as continuous thrust actuators of which the upper bound is related to properties of coils and relative state of the array. A special situation during the maneuver is that the magnetic moment is perpendicular to the relative position. Herein the magnetic force lies in the plane determined by magnetic moment and relative position, and once a vertical maneuver is requested, the satellite might be “stuck”, so corresponding constraints should be taken into consideration.

The magnetic torque acting on the i^{th} satellite due to the j^{th} satellite is:

$$\mathbf{T}_{eij} = \frac{\mu_0 \boldsymbol{\mu}_i}{4\pi} \times [\frac{3\mathbf{r}_{ij}(\boldsymbol{\mu}_j \cdot \mathbf{r}_{ij})}{r_{ij}^5} - \frac{\boldsymbol{\mu}_j}{r_{ij}^3}] \tag{3}$$

The magnetic torque acting on the j^{th} satellite due to the i^{th} satellite is:

$$\mathbf{T}_{eji} = \frac{\mu_0 \boldsymbol{\mu}_j}{4\pi} \times [\frac{3\mathbf{r}_{ij}(\boldsymbol{\mu}_i \cdot \mathbf{r}_{ij})}{r_{ij}^5} - \frac{\boldsymbol{\mu}_i}{r_{ij}^3}] \tag{4}$$

The EM torque is regarded as perturbed moment and in case a feasible control scheme is designed, it can be used as control moment.

2.2 Four-Satellite Planar Formation

Among the stable CW solutions with some geometric properties, the relative orbit of a 3D circle is commonly referred to as the General Circular Orbit (GCO). In case of planar formation, the relative dynamics can be stated concisely. Assuming the distribution of the four-satellite planar formation is symmetrical with respect to the origin of the LVLH coordinate.

Assuming that the equivalent magnet moment and maneuver trajectories are rotational symmetrical, satellites under similar dynamical circumstance are accordant to each other and can be handled in chorus. This ideal scheme for relative orbit transfer is represented in Fig. 1:

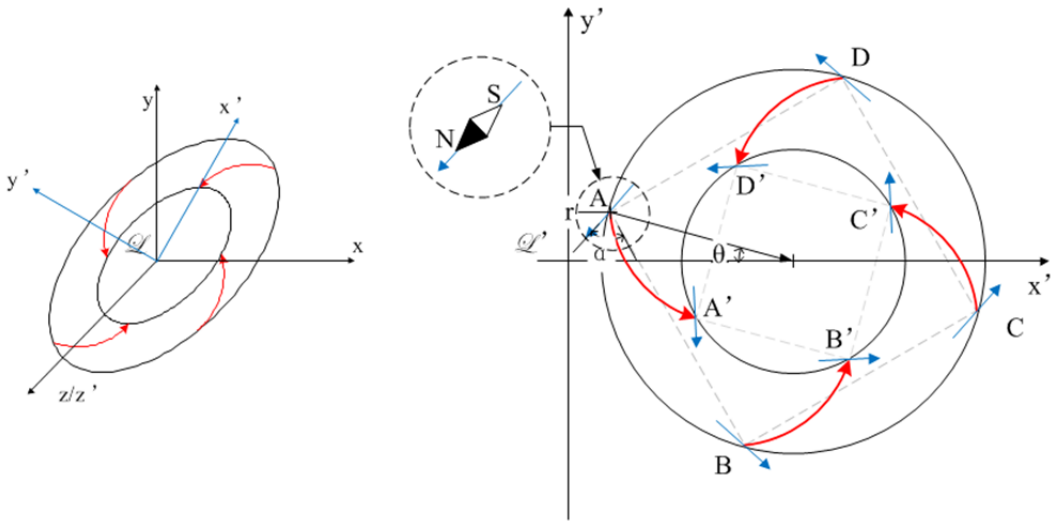

Figure 1. Ideal scheme for relative orbit transfer

where θ_A is the phase angle of satellite A; r_A is the radius of transition orbit; μ_A is the dipole strength and α_A is the deflection angle of dipole moment.

The two-dimensional far-field model (Fig. 2) in the relative frame $\mathscr{R}$ is as follows [6]:

$$\mathbf{F}_{AB} = \frac{3}{4\pi}\frac{\mu_0\mu_A\mu_B}{d^4}[(2\cos\alpha\cos\beta - \sin\alpha\sin\beta)\hat{\mathbf{x}} - (\cos\alpha\sin\beta + \sin\alpha\cos\beta)\hat{\mathbf{y}}] \tag{5}$$

$$\mathbf{T}_A = -\frac{1}{4\pi}\frac{\mu_0\mu_A\mu_B}{d^3}(\cos\alpha\sin\beta + 2\sin\alpha\cos\beta)\hat{\mathbf{z}} \tag{6}$$

$$\mathbf{T}_B = -\frac{1}{4\pi}\frac{\mu_0 \mu_A \mu_B}{d^3}(2\cos\alpha\sin\beta + \sin\alpha\cos\beta)\hat{\mathbf{z}} \tag{7}$$

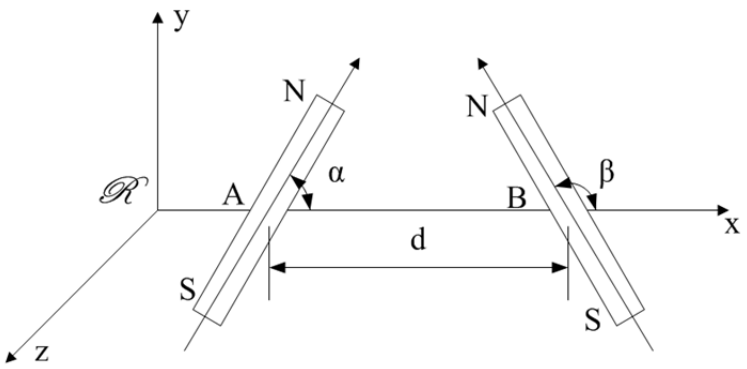

Figure 2. Two-dimensional far-field model

The total EM force acted on satellite A is:

$$\mathbf{F}_A = (\mathbf{F}_{AB})_{R_{AB}} + (\mathbf{F}_{AC})_{R_{AC}} + (\mathbf{F}_{AD})_{R_{AD}} \tag{8}$$

After continuous rotation of coordinate from relative frame $\mathscr{R}_{\mathrm{AC}}$ and $\mathscr{R}_{\mathrm{AD}}$ into the relative frame $\mathscr{R}_{\mathrm{AB}}$ and finally the LVLH frame, the EM force is generally expressed in the form as follows:

$$\mathbf{F}_A = \mathbf{F}_A(\mu_A, r_A, \alpha_A, \theta_A) \tag{9}$$

where $[\mu_A, r_A, \alpha_A, \theta_A]^T$ is the state vector. This description method is concise especially in case of multiple-satellite planar formation.

3 Relative Translational and Rotational Dynamics

The simultaneous control of relative translational and rotational motion demands a 6-DOF model. The relative translational and rotational dynamics is described in the chief-fixed LVLH coordinate $\mathscr{L}$ and deputy's body-fixed frame $\mathscr{B}$ respectively. The coordinates are defined in a routine way.

3.1 Relative Translational Dynamics

In absence of orbital perturbations, equations of relative orbital dynamics expressed in the LVLH frame are as follows:

$$\ddot{\mathbf{r}} = \mathbf{A}_1\mathbf{r} + \mathbf{A}_2\dot{\mathbf{r}} + \mathbf{a} \tag{10}$$

where:

$$\mathbf{A}_1 = \begin{bmatrix} \dot{\theta}^2 + 2\dfrac{\mu}{r_1^3} & \ddot{\theta}^2 & 0 \\ \ddot{\theta} & \dot{\theta}^2 - \dfrac{\mu}{r_1^3} & 0 \\ 0 & 0 & \dfrac{\mu}{r_1^3} \end{bmatrix}, \quad \mathbf{A}_2 = \begin{bmatrix} 0 & 2\dot{\theta} & 0 \\ -2\dot{\theta} & 0 & 0 \\ 0 & 0 & 0 \end{bmatrix}$$

One often normalizes the relative coordinate by the angular velocity to guarantee same magnitude order of the state space.

3.2 Relative Rotational Dynamics

One side effect of applying any shear EM force is introducing shear torque. Owing to the difficulty in solving possible dipole strength, realizing the 6-DOF control merely by accommodating magnetic moment is theoretically. Each satellite is equipped with momentum storage devices so as to be regarded as a fully actuated rotational controller.

Equations for rotational dynamics of the chief satellite are as follows:

$$\dot{\mathbf{q}}_c = \frac{1}{2}\mathbf{q}_c \otimes \begin{bmatrix} 0 \\ \boldsymbol{\omega}_c \end{bmatrix} \tag{11}$$

$$\mathbf{I}_c\dot{\boldsymbol{\omega}}_c + \boldsymbol{\omega}_c \times (\mathbf{I}_c\boldsymbol{\omega}_c) = \mathbf{T}_{ec} + \mathbf{T}_{cc} \tag{12}$$

where $\mathbf{q}_c = [q_{c0}, \mathbf{q}_{cv}^{\mathrm{T}}]^{\mathrm{T}}$ is attitude quaternion; ω_c is the angular velocity in the body-fixed frame; $\mathbf{I}_c$ is the inertia matrix; $\mathbf{T}_{ec}$ is the sum of the EM torque due to other members in the array and is the RW moment. Equations for the i^{th} deputy satellite are as follows:

$$\dot{\mathbf{q}}_i = \frac{1}{2}\mathbf{q}_i \otimes \begin{bmatrix} 0 \\ \boldsymbol{\omega}_i \end{bmatrix} \tag{13}$$

$$\mathbf{I}_i\dot{\boldsymbol{\omega}}_i + \boldsymbol{\omega}_i \times (\mathbf{I}_i\boldsymbol{\omega}_i) = \mathbf{T}_{ei} + \mathbf{T}_{ci} \tag{14}$$

The attitude dynamics of the i^{th} deputy satellite relative to the chief is:

$$\dot{\mathbf{q}}_{ri} = \frac{1}{2}\mathbf{q}_{ri} \otimes \begin{bmatrix} 0 \\ \boldsymbol{\omega}_{ri} \end{bmatrix} \tag{15}$$

where $\mathbf{q}_{ri} = [q_{ri0}, \mathbf{q}_{riv}^{\mathrm{T}}]^{\mathrm{T}}$ is the relative attitude quaternion. The relative angular velocity $\boldsymbol{\omega}_{ri}$ and its time derivative is defined as:

$$\boldsymbol{\omega}_{ri} = \boldsymbol{\omega}_i - \mathbf{A}_{ic}\boldsymbol{\omega}_c \tag{16}$$

$$\dot{\boldsymbol{\omega}}_{ri} = \dot{\boldsymbol{\omega}}_i - \mathbf{A}_{ic}\dot{\boldsymbol{\omega}}_c + \boldsymbol{\omega}_{ri} \times (\mathbf{A}_{ic}\boldsymbol{\omega}_c) \tag{17}$$

where $\mathbf{A}_{ic}$ is the transformation matrix from the chief to the deputy satellite. Combining Eq. 10 and Eq. 11, the relative rotational equation becomes:

$$\begin{aligned} \dot{\boldsymbol{\omega}}_{ri} = &-\mathbf{I}_i^{-1}\{(\boldsymbol{\omega}_{ri} + \mathbf{A}_{ic}\boldsymbol{\omega}_c) \times [\mathbf{I}_i(\boldsymbol{\omega}_{ri} + \mathbf{A}_{ic}\boldsymbol{\omega}_c)]\} + \boldsymbol{\omega}_{ri} \times (\mathbf{A}_{ic}\boldsymbol{\omega}_c) \\ &+\mathbf{A}_{ic}\mathbf{I}_c^{-1}[\boldsymbol{\omega}_c \times (\mathbf{I}_c\boldsymbol{\omega}_c) - (\mathbf{T}_{ec} + \mathbf{T}_{cc})] + \mathbf{I}_i^{-1}(\mathbf{T}_{ei} + \mathbf{T}_{ci}) \end{aligned} \tag{18}$$

Equation 10, 16 and 18 constitute the model of relative translational and rotational dynamics. The coupling among EMFF is reflected implicitly in the connection between EM force and torque. The right side of Eq. 12, 14, marked as T_c and T_i , can be regarded as combined control moment. When $\mathbf{I}_c = \mathbf{I}_i = \mathbf{I} = \mathrm{diag}[I_1, I_2, I_3]$ satisfies $I_1 = I_2 = I_3$, $\mathbf{T}_i - \mathbf{I}\mathbf{A}_{ic}\mathbf{I}^{-1}\mathbf{T}_c = \mathbf{T}_i - \mathbf{A}_{ic}\mathbf{T}_c \triangleq \mathbf{T}_{\Delta ri}$ is defined as the equivalent combined control moment. It contains EM torque and RWs moment and can be optimized to allocate the angular momentum. Omitting *ri* form the subscript, quaternion's second-order derivative is obtained as:

$$\begin{bmatrix} \ddot{q}_0 \\ \ddot{\mathbf{q}}_v \end{bmatrix} = \begin{bmatrix} -\frac{1}{4}(\boldsymbol{\varpi}^{\mathrm{T}}\boldsymbol{\varpi})q_0 - \frac{1}{2}\mathbf{q}_v^{\mathrm{T}}\mathbf{f} - \frac{1}{2}\mathbf{q}_v^{\mathrm{T}}\mathbf{I}^{-1}\mathbf{T}_{\Delta} \\ -\frac{1}{4}(\boldsymbol{\varpi}^{\mathrm{T}}\boldsymbol{\varpi})\mathbf{q}_v + \frac{1}{2}\mathbf{Q}_v\mathbf{f} + \frac{1}{2}\mathbf{Q}_v\mathbf{I}^{-1}\mathbf{T}_{\Delta} \end{bmatrix} \tag{19}$$

where

$$\mathbf{q}_v = [q_1, q_2, q_3]^{\mathrm{T}}$$

$$\mathbf{Q}_v = \begin{bmatrix} q_0 & -q_3 & q_2 \\ q_3 & q_0 & -q_1 \\ -q_2 & q_1 & q_0 \end{bmatrix}, \quad \varpi = \begin{bmatrix} q_0\dot{q}_1 + q_3\dot{q}_2 - q_2\dot{q}_3 - q_1\dot{q}_0 \\ q_0\dot{q}_2 + q_1\dot{q}_3 - q_3\dot{q}_1 - q_2\dot{q}_0 \\ q_0\dot{q}_3 + q_2\dot{q}_1 - q_1\dot{q}_2 - q_3\dot{q}_0 \end{bmatrix}$$

$$\mathbf{f} = \varpi \times (\mathbf{A}_{ic}\boldsymbol{\omega}_c) + \mathbf{A}_{ic}\mathbf{I}^{-1}[\boldsymbol{\omega}_c \times (\mathbf{I}\boldsymbol{\omega}_c)] - \mathbf{I}^{-1}[\mathbf{A}_{ic}\boldsymbol{\omega}_c + \varpi] \times [\mathbf{I}(\mathbf{A}_{ic}\boldsymbol{\omega}_c + \varpi)]$$

$$\mathbf{A}_{ic} = \begin{bmatrix} q_0^2 + q_1^2 - q_2^2 - q_3^2 & -2q_0q_3 + 2q_1q_2 & 2q_0q_2 + 2q_1q_3 \\ 2q_0q_3 + 2q_1q_2 & q_0^2 - q_1^2 + q_2^2 - q_3^2 & -2q_0q_1 + 2q_2q_3 \\ -2q_0q_2 + 2q_1q_3 & 2q_0q_1 + 2q_2q_3 & q_0^2 - q_1^2 - q_2^2 + q_3^2 \end{bmatrix}$$

3.3 6-DOF Relative Dynamics Model

Selecting $\mathbf{x} = [\mathbf{r}^{\mathrm{T}}, \mathbf{q}_v^{\mathrm{T}}]^{\mathrm{T}}$ and $\mathbf{u} = [\mathbf{a}^{\mathrm{T}}, \mathbf{T}^{\mathrm{T}}]^{\mathrm{T}}$ as state and control variables. The coupled translational and rotational dynamics is modeled as:

$$\ddot{\mathbf{x}} = g(\mathbf{x}, \dot{\mathbf{x}}) + \mathbf{C}\mathbf{u} \tag{20}$$

where

$$\mathbf{B}_1 = -\frac{1}{4}(\varpi^{\mathrm{T}}\varpi)\mathbf{q}_v + \frac{1}{2}\mathbf{Q}_v\mathbf{f}, \quad \mathbf{B}_2 = \frac{1}{2}\mathbf{Q}_v\mathbf{I}^{-1}$$

$$g(\mathbf{x}, \dot{\mathbf{x}}) = \begin{bmatrix} \mathbf{A}_1\mathbf{r} + \mathbf{A}_2\dot{\mathbf{r}} \\ \mathbf{B}_1 \end{bmatrix}, \quad \mathbf{C} = \begin{bmatrix} \mathbf{I}_{3\times3} & \mathbf{0} \\ \mathbf{0} & \mathbf{B}_2 \end{bmatrix}$$

4 Optimal Trajectory Generation Using Legendre Pseudospectral Method

Equation 20 is complex in form and contains nonlinear, nonaffine and strong coupling effects, so a direct control law or explicit dipole solution [7] is difficult to achieve. The optimal control problem of trajectory generation is transformed into constrained Non-Linear Program (NLP) through the pseudospectral method [8] and solved through correspondent numerical algorithm.

4.1 Approximating functions

When applying the LPM to continuous optimal control problems, the time interval $[t_0, t_f]$ need to be mapped into the interval $[-1,1]$. An arbitrary function $y(t)$ can be approximated by an N[th] degree polynomial at N+1 interpolation points as follows:

$$y(t) \approx y(t)^N = \sum_{i=0}^{N} y(t_i)\phi_i(t), t \in [-1,1] \tag{21}$$

where t_i is the discretization time, $y(t_i)$ is the interpolation value and $\varphi_i(t)$ is the i^{th} interpolating basis polynomial.
N^{th} degree Legendre orthogonal polynomial can be written as:

$$L_N(t) = \frac{1}{2^N N!} \frac{d^N[(t^2-1)^N]}{dt^N} \tag{22}$$

The N-1 zero points of $\dot{L}_N(t)$ are collocation points. Based on these points, the Lagrangian interpolation polynomials can be written as:

$$\phi_i(t) = \frac{1}{N(N+1)L_N(t_i)} \frac{(t^2-1)\dot{L}_N(t)}{t-t_i} \tag{23}$$

Adopting above polynomials as basis function, the state and control variables can be discretized to approximate the continuous state space. Therefore, the continuous optimal control problem is converted into a NLP problem.

4.2 Optimal Control Problem

4.2.1 State Equation

The original form of system's state equation is Eq. 20 and the corresponding first-order form is:

$$\dot{\mathbf{x}}(t) = F(\mathbf{x}(t), \mathbf{u}(t), t) \tag{24}$$

The discretized form is:

$$\sum_{i=0}^{N} D_{ki}\mathbf{x}_i - \frac{t_f - t_0}{2} F(\mathbf{x}^N(t_k), \mathbf{u}^N(t_k), t_k; t_0, t_f) = 0, k = 0,1,2,\ldots,N \tag{25}$$

where D is an (N+1)×(N+1) matrix.

4.2.2 Control Constraints

There is a host of constraints needed to be considered, including constraints on control output, path, energy matching, configuration and bound conditions. The constraints on control output include saturation of both magnetic moment and RW control torque while the former is a function of immediate relative state of satellites. The path constraints involve assumptions of far-field model, anti-“stuck” conditions and collision avoidance. Constraints on energy matching, configuration and bound conditions are directed to initial and terminal conditions.

4.2.3 Cost Function

The cost functions of relative translational control, AMM optimization problem and control output are defined as:

$$J_{trans.} = \min(T_f - T_0) \tag{26}$$

$$J_{rot.} = \min \sum_{i=1}^{N_{sat}} \mathbf{T}_{ci}^T \mathbf{W}_{Ti} \mathbf{T} c_i \tag{27}$$

$$J_{ctl.} = \min \sum_{i=1}^{N_{sat}} \sum_{k=1}^{N} [\boldsymbol{\mu}_i(t_{k+1}) - \boldsymbol{\mu}_i(t_k)]^T \mathbf{W}_{\mu i} [\boldsymbol{\mu}_i(t_{k+1}) - \boldsymbol{\mu}_i(t_k)] \tag{28}$$

where $\boldsymbol{\mu}(\tau_k)$ is the vector of dipole value at the time step τ_k, $\mathbf{W}_{\mu i}$ is the weighting matrix for differential dipole value and $\mathbf{W}_{Ti}$ is the weighting matrix for control moment of the i[th] satellite. The cost function is set to accomplish the following objectives:

(1) Firstly it tries to avoid frequent switch of dipole polarity. [9] points out that changing the sign of both dipoles does not affect the force between two dipoles. Due to inherent hysteresis of magnet, a smooth change in dipole strength is requested.

(2) Secondly it tries to distribute the control moment “evenly” among the formation, so the synchronous off-load of RWs can be achieved by switching dipole polarity. The RW angular momentum constraints are initially expressed in the form of integral inequality and here a quadric term is replaced.

The general control problem is described as follows:

$$
\begin{aligned}
&\min J = J_{trans.} + J_{rot.} + J_{ctl.} \\
&\text{Subject to:} \\
&\textbf{Equality constraints:} \\
&\quad \text{Dynamics:} && \begin{cases} v(\tau) = \dot{x}(\tau) \\ \dot{v}(\tau) = g(x, v, \tau) + C(x, \tau)u(\tau) \end{cases} \\
&\quad \text{Enenrgy matching:} && h_1(x(\tau_f), \tau_f) = 0 \\
&\quad \text{Configuration:} && h_2(x(\tau_f), \tau_f) = 0 \\
&\quad \text{Initial and terminal conditions:} && \begin{cases} h_0(x(\tau_0), \tau_0) = 0 \\ h_f(x(\tau_f), \tau_f) = 0 \end{cases} \\
&\textbf{Inequality constraints:} \\
&\quad \text{Control output:} && g_1(x(\tau), u(\tau), \tau) \geq 0 \\
&\quad \text{Anti-"stuck" conditions:} && g_2(x(\tau), u(\tau), \tau) \geq 0 \\
&\quad \text{Collision avoidance:} && g_3(x(\tau), u(\tau), \tau) \geq 0
\end{aligned}
\tag{29}
$$

5 Numerical Computation Method and Simulation Results

5.1 Numerical Computation Method

Without using any toolbox, this constrained NLP can be solved in a numerical way which can be used to solve similar optimization problems. The resulting constrained NLP can be transformed into an unconstrained one through the generalized Lagrangian multiplier method. During the process of searching, the state space is modified to minimize the penalty function which contains the cost function and constraints through the quasi-Newton method. The search direction is determined by gradient of the penalty function and the Hessian matrix; the latter one generated by a single algorithm may be unsteady and will affect the convergence rate. In this paper, a new method, namely the integrated DFP, is applied. A switch of original DFP and BFGS can reach higher accuracy and faster convergence rate under reduced computation complexity. Comparing several methods of one-dimensional search, the modified pattern search method is adopted to determine the search step. The weakness of other algorithms, like the golden section search and cubic interpolation method, can be obvious due to the complex character of penalty function's derivative. The procedure for solving the NLP is summarized as follows:

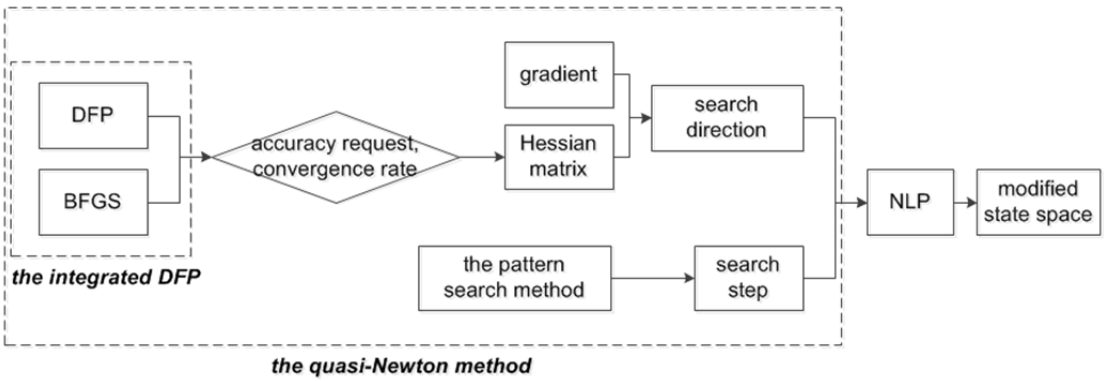

Figure 3. The procedure for solving the NLP

5.2 Simulation Results

In order to verify the validity of the proposed optimization method, a 6-DOF NLP is built on the platform of Microsoft Visual Studio 2010. Without using any current commercial optimization software, the frame of four-satellite planar formation on the GCO is simulated. The simulation results are as follows.

Parameters used in the simulation are listed in Tab. 1.

Table 1. Parameters used in the simulation

Parameter	Value	Parameter	Value
Mass of satellite (kg)	250	Radius of initial reference orbit (km)	7200
I (kg·m^2)	160	Radius of terminal reference orbit (km)	7200
Radius of initial GCO (m)	10	Maximum magnet moment (H/m)	162500
Radius of terminal GCO (m)	5	Maximum RW torque (N·m)	1

The initial and terminal relative nominal trajectory is set as:

$$\begin{cases} x_i = 5\sin(n_i t + \beta_i) \\ y_i = 10\cos(n_i t + \beta_i) \\ z_i = 5\sqrt{3}\sin(n_i t + \beta_i) \end{cases} \qquad \begin{cases} x_f = 5\sin(n_f t + \beta_f) \\ y_f = 10\cos(n_f t + \beta_f) \\ z_f = 5\sqrt{3}\sin(n_f t + \beta_f) \end{cases}$$

The initial relative quaternion is set as $\mathbf{q}_{vi} = [-0.7, 0.5, -0.2]^T$.

The formation reconfigures for the purpose of transferring to another relative orbit while keeping the square configuration. When the initial and terminal phase angles of relative orbit are fixed, the simulation results is suboptimal and may lead to extreme control indicated by simulation results; β_i and β_f, as well as state and control vectors, can be optimized. The reconfiguration is limited to the maneuver plane and results are shown in Fig. 4, 5 and 6. The optimal maneuver time is about 151.78 seconds.

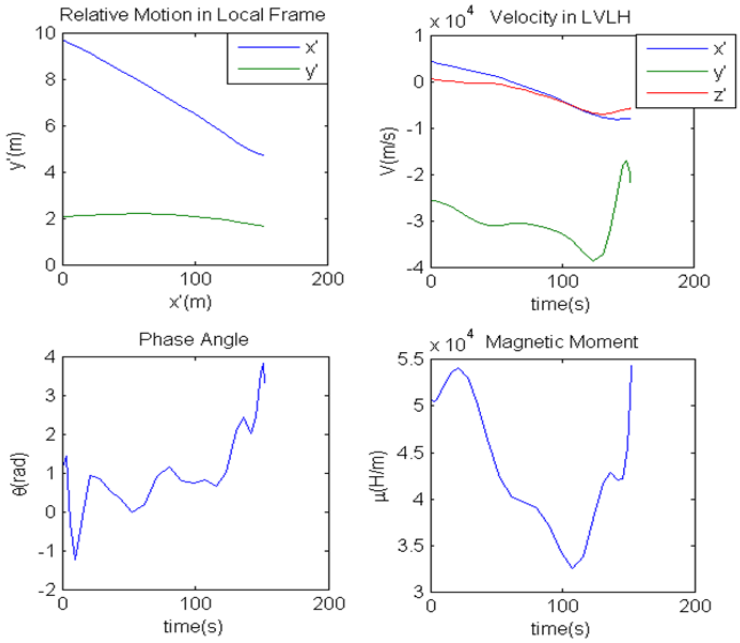

Figure 4. State and control results of satellite A

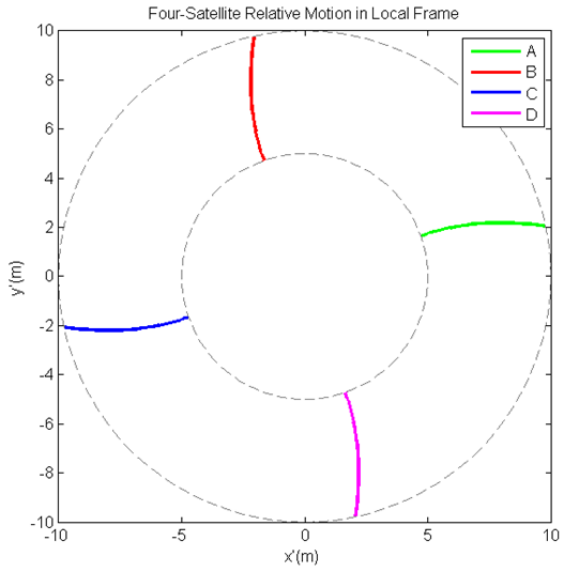

Figure 5. Relative motion of four-satellite planar reconfiguration

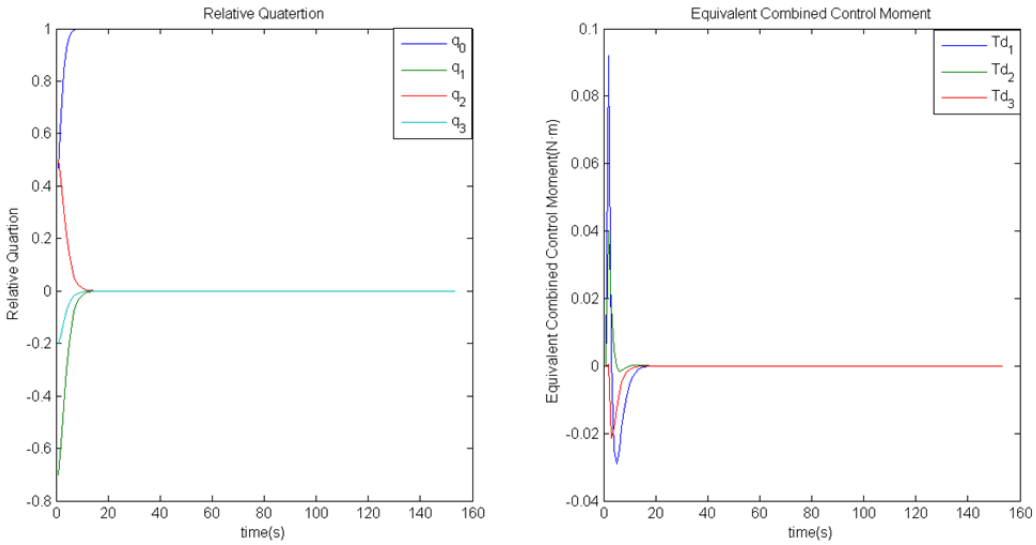

Figure 6. Relative translation of four-satellite planar reconfiguration

The simulation indicates that the model of relative translational dynamics in not only complicated in the form, but also the characteristic of is derivative. The modification of relative quaternion is difficult, so the selection of initial intermediate state can be based on certain control law, e.g. the PID method. It can be concluded that the satellite firstly tries to track the relative attitude and then tries to counteract the influence of EM torque.

Simulation results of satellite A's maneuver using the state feedback control are shown in Fig. 5. Compared with results as showed above, the requested magnetic moment is extremely large, even beyond the upper limit. Moreover, large EM torque, acting as disturbance, leads to difficulty in attitude stabilization. The results indicate that this control method is not applicable especially for the case of scaled-down reconfiguration because of slight magnitude of initial EM force.

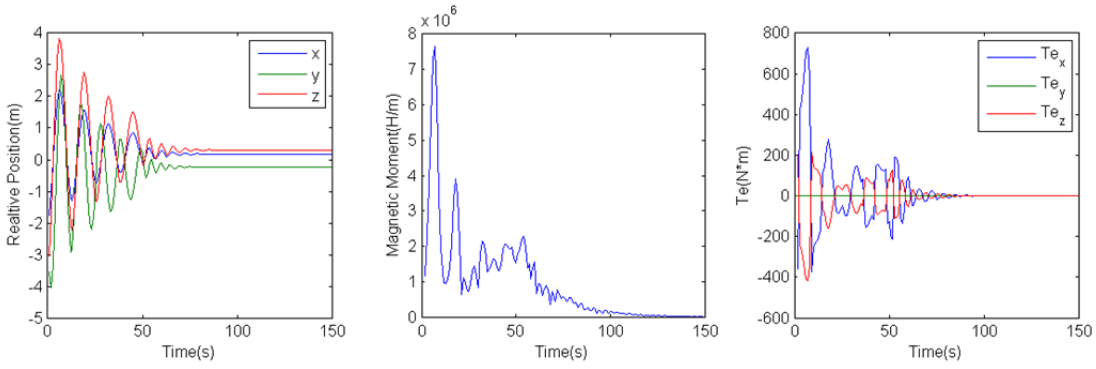

Figure 7. Four-satellite planar reconfiguration using state feedback

6 Conclusions

A 6-DOF relative motion model is applied to fully utilize the inherent coupling EM effects. In this paper, the Legendre Pseudospectral Method (LPM), as well as its high-precision numerical computation method, is used to generate optimal trajectories. The simulation results verify the validity of the proposed optimization method and numerical algorithm.

Due to the conservation of mechanical energy and total angular momentum, the 6-DOF dynamic model can be derived in an analytical mechanics approach. The simulation results indicate that the initial and terminal conditions will affect convergence rate and selection of parameters can influence the precision of simulation. A series of algorithm with high fidelity and fast convergence rate can be applied to similar optimal control problem.

7 Acknowledgements

The authors wish to thank gratefully National Key Laboratory of Aerospace Flight Dynamics in Northwestern Polytechnical University, Xi'an, China, for their support. This work is supported by the National Natural Science Foundation of China (11172235) and Innovation Foundation of Shanghai Aerospace Science and Technology.

8 References

[1] Umair, A., David, W. M., and Jaime, L. R., "Control of Electromagnetic Satellite Formations in Near-Earth Orbits", Journal of Guidance, Control, and Dynamics, Vol. 33, No. 6, 2010, pp. 1883-1891.

[2] DANIEL, W. K., "Electromagnetic Formation Flight of Satellite Arrays", Master's Thesis, Massachusetts Institute of Technology

[3] Y.W. Zhang, Le. P. Yang, Y. W. Zhu, X. H. Ren and H. Huang., "Self-docking capability and control strategy of electromagnetic docking technology", Acta Astronautica, 69 (2011) 1073–1081.

[4] G. Q. Zeng, M. Hu, "Finite-time control for electromagnetic satellite formations", Acta Astronautica, 74 (2012) 120–130.

[5] Roman, W., Marek, B., and Karol, S., "Autonomous Reconfiguration of Servicing Satellite by Electromagnetic Forces", 9th ESA Workshop on Advanced Space Technologies for Robotic and Automation.

[6] Daniel, W. K., Raymond, J. S., and Aya S., "Micro-Electromagnetic Formation Flight of Satellite Systems", AIAA SPACE 2010 Conference & Exposition.

[7] Samuel, A. S., and Raymond, J. S., “Explicit Dipole Trajectory Solution for Electromagnetically Controlled Spacecraft Clusters”, Journal of Guidance, Control, and Dynamics, Vol. 33, No. 4, 2010, pp. 1225-1235.

[8] Geoffrey, T. H., and Anil, V. R., “Optimal Reconfiguration of Spacecraft Formations Using the Gauss Pseudospectral Method”, Journal of Guidance, Control, and Dynamics, Vol. 31, No. 3, 2008, pp. 689-698.

[9] Umair A., “Dynamics and Control of Electromagnetic Satellite Formations”, Master’s Thesis, Massachusetts Institute of Technology